APRIL 1983

LIDS-P-1346

CONIC SECTOR ANALYSIS OF SAMPLED-DATA FEEDBACK SYSTEMS*

Peter M. Thompson - Department of Electrical Engineering
California Institute of Technology
Pasadena, CA 91125 USA

Gunter Stein - Laboratory for Information and Decision Systems
Michael Athans Massachusetts Institute of Technology
Cambridge, MA 02139, USA

ABSTRACT

A multivariable sampled-data feedback system contains a digital computer embedded in a sampled-data compensator that controls an analog system. Conic sectors that can be used to analyze this feedback system are presented, and then it is shown how to use them to determine closed loop stability and to analyze robustness. These conic sector analysis techniques are an alternative to z-transform techniques. They directly incorporate the prefilter, sample rate, and hold device in the analysis, and allow the sampled-data feedback system to be rigorously approximated by a linear time invariant feedback system.

---

*This research was carried out at the M.I.T. Laboratory for Information and Decision Systems with support provided by NASA under grant NGL-22-009-124 and by the General Electric Corporate Research and Development Center.

This paper has been prepared for the 9th IFAC Congress in July, 1984.

I. INTRODUCTION

Digital computers are commonly used to control analog systems. Examples can be found across the spectrum of engineering disciplines, especially in the aerospace industry, where they have been used to control aircraft, helicopters, missiles, and spacecraft. Digital computers have won wide acceptance for a variety of reasons including cost, reliability, and flexibility. Here we are primarily concerned with the ability of digital computers to mimic analog compensators, despite their "sampled-data" nature.

Most analysis and design techniques for sampled-data control systems are based on the use of z-transforms, as explained in many textbooks including the one by Franklin and Powell [1]. In this paper, we introduce new analysis techniques that are based on the use of conic sectors, which were developed for a general class of feedback systems by Zames [2] and Safonov [3,4].

The sampled-data compensator consists of a prefilter, synchronous sampler, digital computer, and hold device and can be modeled as a linear time varying (LTV) transformation from its input to its output. This transformation can be approximated by a linear time invariant (LTI) transformation, thereby allowing the use of Laplace transform matrices. Conic sectors are used to make this a rigorous approximation, by which we mean an approximation that is valid for all possible inputs. The center and radius of the conic sector, or cone, are used to determine closed loop stability and various robustness margins.

It is well known that sampled-data compensators behave like LTI compensators for low frequency ($< \frac{\pi}{T}$ rad/sec) inputs but not for high frequency inputs. This fuzzy idea is made precise by characterizing the uncertain high frequency behavior as a frequency dependent modeling error, i.e. as the radius of a cone. When this is done then it can be treated as are other frequency dependent modelling errors, such as unmodelled high frequency dynamics, structural resonances, unmodelled time delays, and the like. It is the subject of robustness to show that stability is preserved in spite of these modelling errors. The usual design procedure for doing so; which is at least as old as Nyquist and Bode, God rest their souls, and Nichols, may he live long and prosper; is to roll off the loop transfer function at high frequencies.

One of the problems with existing z-transform theory is its inability to justify the need for prefiltering. Stability, robustness margins, and performance constraints can all appear marvelous even with no prefiltering! The problem of selecting the prefilter and also the problem of selecting the sample rate are well known, and from a practical engineering point of view solved, but the theory still lags behind. Our approach offers the advantage of directly incorporating the prefilter, sample rate, and hold device into the analysis, because they all affect the frequency dependent modeling error.

This paper is an exposé of research in this subject conducted over the last several years at MIT's Laboratory for Information and Decision Systems. Previous publications [5, 6, 7, 8] are referenced where appropriate. We begin in Section II by setting up in sufficient generality the conic sector analysis techniques. In Section III these are particularized to sampled-data control systems. This involves the foremost result to data (Lemma 5) - the discovery of a new conic sector that contains a sampled-data operator. In Sections IV, V, and VI three different techniques for applying this new conic sector are described. The ability to determine closed loop stability and to measure robustness margins is demonstrated in examples. The effect of varying the sample rate is explored. In Section VII future research is discussed and conclusions are presented.

II. MATHEMATICAL PRELIMINARIES

We establish notation, define the sampled-data control system, and then review conic sector sufficient conditions for closed loop stability. We make a few qualitative statements about conic sectors and then review how they can be applied to LTI operators.

Notation

R^n, C^n, R^{nxm}, C^{nxm} = finite dimensional real and complex Euclidean spaces

L_2^n = n-dimensional space of square integrable functions

L_{2e}^n = extended L_2^n space

$\underline{A} \in C^{nxm}$ = matrix (underlined capital Roman letters)

$\underline{a} \in C^n$ = vector (underlined small Roman letters)

$a, \alpha \in C$ = scalars (small Roman and Greek letters)

$A \subset L_{2e}^n \times L_{2e}^m$ = relation or operator (capital script letters)

$\underset{\sim}{a} \in L_{2e}^n$ = vector of functions (small Roman letters underlined by a tilda)

$\underline{A}^{-1}$ = matrix inverse

A^I = inverse of relation or operator

$||\underline{a}||_E$ = Euclidean vector norm

$||\underline{A}||$ = matrix norm induced by Euclidean vector norm

$||\underset{\sim}{a}||_\tau$ = truncated function norm

$||A||$ = operator norm induced by truncated function norm

$\sigma_{max}(\underline{A}) = ||\underline{A}||$ = maximum singular value of $\underline{A}$

$\sigma_{min}(\underline{A})$ = minimum singular value of $\underline{A}$

Abbreviations:

R_+ = real numbers ≥ 0

$\underline{F}_k = \underline{F}(jw-jw_s k)$, where $w_s = 2\pi/T$

$\underline{D}^* = \underline{D}(z)$ evaluated at $z=e^{j\omega T}$

$\sum_k(\cdot)$ = sum from $k = -\infty$ to ∞

$\sum_{k\neq n}(\ )$ = sum from $k = -\infty$ to ∞ except the $k=n$ term

■ = end of statement of Lemma or Theorem

Particular operators associated with sampled-data control system:

$\tilde{K}$ = sampled-data operator (LTV)

$\tilde{G}$ = plant operator (LTI)

$\tilde{T}$ = loop transfer operator (LTV)

K,R = center and radius of cone that contains $\tilde{K}$ (LTI operators)

G, R_g = center and radius of cone that contains $\tilde{G}$ (LTI operators)

T, R_t = center and radius of cone that contains $\tilde{T}$ (LTI operators)

Associated with each LTI operator A is the Laplace transform matrix $\underline{A}(s)$, and with each function $\underset{\sim}{a}$ the Laplace transform $\underline{a}(s)$. Associated with the

sampled-data operator $\tilde{K}$ are the Laplace transform matrices $\underline{F}(s)$ and $\underline{H}(s)$, the z-transform matrix $\underline{D}(z)$, and the sample period of T seconds. The Laplace transforms are often evaluated on the imaginary axis, $s = j\omega$ and the z-transforms on the unit circle, $Z = e^{jwt}$.

The Sampled-Data Control System

A block diagram of the multivariable sampled-data feedback system is shown in Figure 1. The nominal plant is modeled by the Laplace transform matrix $\underline{G}(s)$. Frequency dependent modeling errors are characterized by the multiplicative perturbation $\underline{E}_m(s)$, and the actual plant is

$$\tilde{\underline{G}}(s) = \underline{G}(s)\,[\underline{I} + \underline{E}_m(s)] \tag{1}$$

$$\sigma_{max}[\underline{E}_m(j\omega)] < \ell_m(\omega) \quad \text{for all } \omega \tag{2}$$

The multiplicative perturbation is unstructured because the only information known about it is a bound on its maximum singular value. For information on singular values see [9,10] and their references.

The sampled-data compensator contains a prefilter, computer, and hold device which are modelled, respectively, by $\underline{F}(s)$, $\underline{D}(z)$, and $\underline{H}(s)$. The single synchronous sampler outputs new samples every T seconds. The transformation from the error signal $\underline{e}(s)$ to the plant input $\underline{u}(s)$ is a LTV transformation defined by

$$\underline{u} = \underline{H}\,\underline{D}^*\,\frac{1}{T}\,\sum_k \underline{F}_k\,\underline{e}_k \tag{3}$$

The closed loop transformation from the command input $\underline{r}(s)$ to the plant output $\underline{y}(s)$ is the following:

$$\underline{y} = \underline{G}\,\underline{H}\,\underline{D}^*_{cl}\,\frac{1}{T}\,\sum_k \underline{F}_k\,\underline{e}_k \tag{4}$$

where

$$\underline{D}^*_{cl} = \underline{D}^*\,(\underline{I} + \underline{G}^*_d\,\underline{D}^*)^{-1} \tag{5}$$

$$\underline{G}^*_d = \frac{1}{T}\,\sum_k \underline{F}_k\,\underline{G}_k\,\underline{H}_k \tag{6}$$

The z-transform $\underline{G}_d(z)$ is the discretized plant.

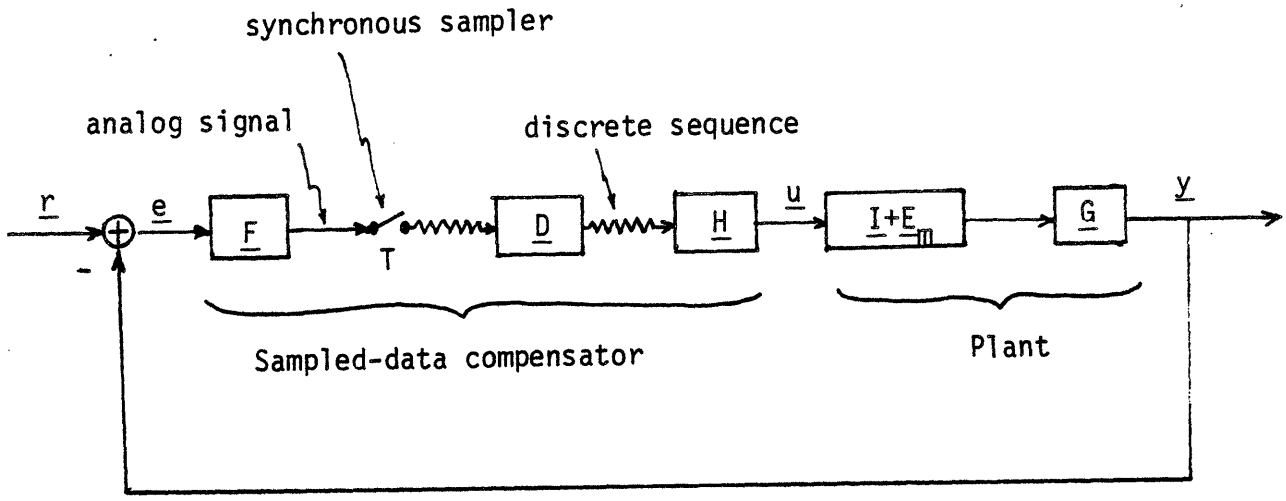

Figure 1: The sampled-data feedback system

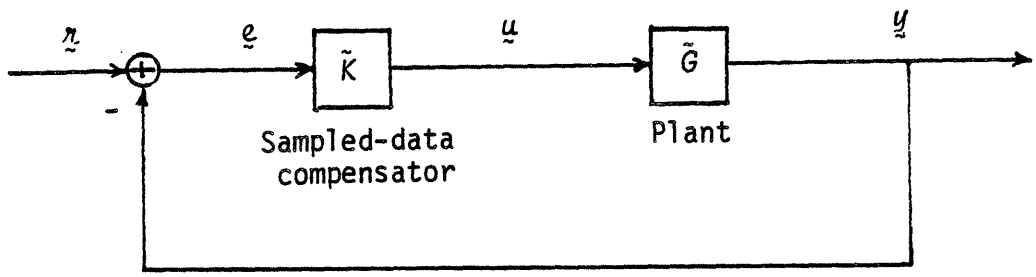

Figure2: Then sampled-data feedback system, represented with operator notation

Conic Sectors

The most general application of conic sectors gives sufficient conditions for closed loop stability of nonlinear, time-varying, noncausal, and ill-posed control systems. The elements of the control systems are relations defined as cross products on extended normed linear spaces. We don't need all of this blazing generality, and quickly descend to the sampled-data control system of Figure 2, which is the same as Figure 1, except that operator notation is used. The plant $\tilde{G}$ is a LTI operator with the transformation defined by (1). The compensator $\tilde{K}$ is a LTV operator with the transformation defined by (3).

We now present some standard definitions all of which are further discussed in [2], [3], [4], and [7]. A "relation" is a subset of the cross product space $L_{2e}^m \times L_{2e}^r$. An "operator" is a special case of relation that satisfies the 2 properties that (1) their domains are all of L_{2e}^m and (2) for every input there exists a unique output. The only extended normed linear space used in this paper is L_{2e}^m. Its elements are square integrable m-dimensions functions $\underset{\sim}{x} : R_+ \rightarrow R^m$, from the set of real numbers ≥ 0 to the set of m-dimensional vectors, such that for all $\tau \in R_+$ they have finite truncated norms:

$$||\underset{\sim}{x}||_\tau^2 \triangleq \int_0^\tau ||\underset{\sim}{x}(t)||_E^2 dt \qquad (7)$$

The extended space and its truncated norm are used so that both stable and unstable relations are defined in the same way.

Let A be an arbitrary operator. The input-output pair $(\underset{\sim}{x}, \underset{\sim}{y}) \in A$ can equivalently be denoted by the transformation $\underset{\sim}{y} = A\underset{\sim}{x}$. The "gain" of the operator A is defined

$$||A|| \triangleq \sup \frac{||A\underset{\sim}{x}||_\tau}{||\underset{\sim}{x}||_\tau} \qquad (8)$$

where the suprenum is taken over all $\underset{\sim}{x}$ in the domain of A and all $\tau \in R_+$ such that $||\underset{\sim}{x}||_\tau \neq 0$. If the gain of A is finite then it is "L_{2e}-stable". The "inverse" of the operator A always exists, though it may be a relation and not an operator, and is defined by

$$A^I = \{ (\underset{\sim}{x},\underset{\sim}{y}) \in L_{2e}^r \times L_{2e}^m \mid (\underset{\sim}{x},\underset{\sim}{y}) \in A \} \qquad (9)$$

The composite operators $A + B$, AB, $A-B$ are more-or-less obviously defined. The unity operator is I.

There are two different definitions given for conic sectors. The relation A is "strictly inside cone (C,R)" with center C and radius R if

$$||\underset{\sim}{y} - C\underset{\sim}{x}||_\tau^2 \leq ||R\underset{\sim}{x}||_\tau^2 - \varepsilon ||\underset{\sim}{x}||_\tau^2 \qquad (10)$$

for all $(\underset{\sim}{x},\underset{\sim}{y}) \in A$, all $\tau \in R_+$, and some $\varepsilon > 0$. In contrast to (10), the relation A is "outside cone (C,R)" if

$$||\underset{\sim}{y} - C\underset{\sim}{x}||_\tau^2 \geq ||R\underset{\sim}{x}||_\tau^2 \qquad (11)$$

for all $(\underset{\sim}{x},\underset{\sim}{y}) \in A$ and all $\tau \in R_+$.

The radii that we will use will always have the property that both R and R^I are LTI L_{2e}-stable operators. This implies that the Laplace transform matrix $\underline{R}(s)$ associated with R has all of its poles and zeros in the left-half-plane and does not roll off at high frequencies (i.e. $\underline{R}(s) \to \underline{0}$ as $s \to \infty$).

Referring now to the control system of Figure 2, it is assumed to be causal and well-posed, which is equivalently stated, thanks to Willems [11], that $(I + \tilde{G}\tilde{K})^I$ is a causal operator. Define F and E to be closed loop operators which transform $\underset{\sim}{r}$ to $\underset{\sim}{e}$ and $\underset{\sim}{u}$, respectively. The closed loop system is stable if both F and E and L_{2e}-stable. A sufficient condition for this to be true is given by the "Small Gain Theorem" [2]:

$$||\tilde{\tilde{G}}\tilde{K}|| \leq 1-\varepsilon \quad \text{for some } \varepsilon > 0 \qquad (12)$$

As everyone knows, or at least should know, this condition is too restrictive to be of any but theoretical interest. Modifications using conic sectors, however, are indeed useful. It can be argued, somewhat facetiously, that the following conic sector stability conditions, indeed all of [2], [3], and [4], are but trivial consequences of a trivial theorem.

The closed box system of Figure 2 is stable if there exists a cone (K,R) such that

$$\begin{aligned} &\tilde{K} \text{ is strictly inside cone } (K,R) \\ &-\tilde{G}^I \text{ is outside cone } (K,R) \end{aligned} \tag{13}$$

Similarly, by switching the roles of $\tilde{G}$ and $\tilde{K}$, another sufficient condition for closed loop stability is

$$\begin{aligned} &\tilde{G} \text{ is strictly inside cone } (G,R) \\ &-\tilde{K}^I \text{ is outside cone } (G,R) \end{aligned} \tag{14}$$

It is arbitrary how the elements of the control system are divided. Let $\tilde{T}$ be the loop transfer operator for the loop broken at any point, and then it follows that the closed loop system is stable if

$$\begin{aligned} &\tilde{T} \text{ is strictly inside cone } (T,R) \\ &-\tilde{I} \text{ is outside cone } (T,R) \end{aligned} \tag{15}$$

The cone can be considered a "topological separation" between elements of the control system. It is this idea of topological separation that leads to the further generalizations of Safonov [4].

An important point to be made is that the conic sector stability results are also robustness results. They determine stability not just for particular operators $\tilde{G}$ and $\tilde{K}$ but for any such operators that satisfy the conic sector conditions.

Some Insight

Having worked for some time with conic sectors we offer the following qualitative information. Consider when the operator A is strictly inside cone (C,R). The center C is an approximation of A. If C is to be a useful approximation then it should be simple (i.e. linear time invariant) and in some sense close to A, at least for a certain class of input signals, the most useful being low frequency sinewaves. A trivial cone always exists by making the radius infinitely large. Nontrivial cones exist when the operator $A-C$ is L_{2e}-stable. The radius R should be as small as possible.

The radius is intuitively a bound on the errors of the approximation C, abstractly an additive pertubation, and precisely a bound on the energy of certain signals. The truncated function norm is proportional to the energy of the truncated signal. Therefore the conic sector inequality (10) can be stated that the energy of $(A-C)\underset{\sim}{x}$ is less than the energy of $R\underset{\sim}{x}$ for all possible $\underset{\sim}{x}$.

Next consider when $-A^I$ is outside cone (C,R). It is not useful to think of C, or anything else, as an approximation of A. More useful is to consider the feedback system with A in the feedforward position and C in the feedback position. If this feedback system is well-posed and closed loop stable then the condition that $-A^I$ is outside cone (C,R) is equivalent to the condition that the gain of $RA\ (I+CA)^I$ is < 1.

In all robustness work a nominal system is defined and then assumed or shown to be stable. If $-A^I$ is outside cone (C,R) then the nominal system has the loop transfer operator CA. If both C and A are LTI then so is the nominal system.

Conic Sectors for LTI Control Systems.

We will use the following three Lemmas, which show how conic sectors are applied to LTI operators. Lemma 1 gives sufficient conditions for a LTI operator $\tilde{G}$ to be strictly inside of a cone.

Lemma 1. Define the LTI operators $\tilde{G}$, G, and R_g. Assume that R_g^I is also a LTI operator, and that R_g and R_g^I are L_{2e}-stable. Then $\tilde{G}$ is strictly inside cone (G,R_g) if

(i) $\tilde{G}-G$ is L_{2e}-stable

(ii) $$\sigma_{min}[\underline{R}_g(j\omega)] > \frac{1}{(1-\varepsilon)^{1/2}}\ \sigma_{max}\ [\underline{\tilde{G}}(j\omega)-\underline{G}(j\omega)]$$

for all ω and some $\varepsilon > 0$ ■ (16)

A proof of Lemma 1 is contained in [4]. If the uncertainty of the plant $\tilde{G}$ is characterized by a multiplicative perturbation as in (1), then $\tilde{G}$ is strictly inside of a cone with center G and radius R_g, for any R_g such that

$$\sigma_{min}[\underline{R}_g(j\omega)] \geq \frac{1}{(1-\varepsilon)^{1/2}}\ \ell_m(\omega)\ \sigma_{max}[\underline{G}(j\omega)]$$

for all ω and some $\varepsilon > 0$ (17)

The next Lemma gives sufficient conditions for a LTI operator G to satisfy the property that $-G^I$ is outside of a cone. It is also proved in [4]. The assumption that $(I + KG)^I$ is a LTI operator is for well-posedness. Condition (i) can be thought of as a condition that the nominal LTI is closed loop stable, and can be checked by a variety of well known techniques.

Lemma 2. Define the LTI operators G, K, and R. Assume that R^I and $(I + KG)^I$ are LTI operators. Then $-G^I$ is outside cone (K,R) if

$$\begin{aligned} &\text{(i)} \quad G(I+KG)^I \text{ is } L_{2e}\text{-stable} \\ &\text{(ii)} \quad \sigma_{max}[\underline{R}\ \underline{G}\ (\underline{I}+\underline{G}\ \underline{K})^{-1}(j\omega)] \leq 1 \text{ for all } \omega \end{aligned} \qquad (18)$$

■

The third Lemma is a combination of the previous two. The LTI operator $\tilde{G}$ is strictly inside of a cone which has a radius that satisfies (16) and (17). Sufficient conditions were given for all possible $\tilde{G}$'s strictly inside of this cone to be outside of another cone. The proof is presented in Appendix A.

Lemma 3. Define the LTI operators $\tilde{G}$, G, and R_g, and assume that $\tilde{G}$ is strictly inside cone (G, R_g), as shown in Lemma 1. In addition, define the LTI operators K and R, and assume that $-G^I$ is outside cone (K,R), as shown in Lemma 2. For all allowable $\tilde{G}$'s it follows that $-\tilde{G}^I$ is outside cone (K,R) if

$$\ell_m(\omega) < \frac{\sigma_{min}[\underline{I} + \underline{K}\ \underline{G}\ (j\omega)] - \sigma_{max}[\underline{R}\ \underline{G}\ (j\omega)]}{\sigma_{max}[\underline{K}\ \underline{G}\ (j\omega)] + \sigma_{max}[\underline{R}\ \underline{G}\ (j\omega)]} \text{ for all } \omega \quad \blacksquare \qquad (19)$$

This completes the section of mathematical preliminaries. We are now ready to apply conic sectors to sampled-data control systems.

III. Conic Sectors for Sampled-Data Operators

The task before us is to show the existence of a useful cone that contains the sampled-data operator $\tilde{K}$. To be useful, this cone must be computable and result in non-conservative sufficient conditions for closed loop stability and robustness. In this section we discuss three different cones. It is argued that the first two fail the test of usefulness. The next three sections of this paper are used to argue that the third cone is indeed useful.

We emphasize the distinction between showing existence and showing usefulness. We know, for instance, that the trivial cone with an infinitely large radius always exists. We also know, for instance, that this cone is not in the least bit useful.

The first non-trivial cone was found by Kostovetsky [5,6]. He considered a very specific type of sampled-data operator which he named the "optimal hybrid approximation." Its prefilter, computer, and hold are chosen to minimize the mean square difference of the outputs of the sampled-data and LTI operators when the input is white noise. This turns out not to be a practical compensator because the prefilter, computer, and hold all contain internal models of the LTI operator. Because this cone only applies to the optimal hybrid approximation we do not consider it to be a useful cone, and we will not further discuss it. We nonetheless applaud the pioneering efforts of its founder.

The second cone was found by Stein and reported in [6]. It is a generalization of the first cone that can be applied to any L_{2e}-stable $\tilde{K}$. The center K is arbitrary, though it should in some sense be close to $\tilde{K}$, and the radius R is the non-dynamic scalar multiplier $\underline{R}(s) = r\underline{I}$. The result is stated below as Lemma 4. Its proof and a discussion of the impulse response $\tilde{K}(t,\theta)$ are contained in [6].[1]

Lemma 4. Define the sampled-data operator $\tilde{K}$, the LTI operator K, and their respective impulse response matrices $\underline{\tilde{K}}(t,\theta)$ and $\underline{K}(t-\theta)$. Assume both are L_{2e}-stable. $\tilde{K}$ is strictly inside cone (K,R) if $\underline{R}(s) = r\underline{I}$, where

$$r = \| M \| = m(s)\Big|_{s=0} = \int_0^\infty m(t)dt \tag{20}$$

[1] Lemma 4 is true not just for the sampled-data operator $\tilde{K}$ but for any LTI operator $\tilde{K}$.

where

$$m(t-\theta) \geq \frac{1}{(1-\varepsilon)^{1/2}} \sigma_{max}[\underline{\tilde{K}}(t,\theta)-\underline{K}(t-\theta)]$$

for all t,θ and some $\varepsilon > 0$ ■ (21)

Computing r involves a difficult maximization over both t and θ. A lower bound for T is

$$r \geq \sigma_{max}[\underline{K}(j\omega)] \text{ evaluated at } \omega = \frac{\pi}{T} \tag{22}$$

which is explained by the fact that a sinewave input at π/T rad/sec can result in zero output.

This second cone fails the test for usefulness because it is difficult to compute. Even if we were clever enough to find an easy way to compute r, the cone is not useful because of the more serious reason that any cone with a nondynamic radius will result in conservative sufficient conditions for closed loop stability. This conservativeness can be shown by example, or explained intuitively as follows. The scalar multiplier r must be large to bound the significant differences in the outputs of $\tilde{K}$ and K in response to high frequency inputs. This same value of r will be a conservative (i.e. too large) bound for low frequency inputs, which in turn results in conservative sufficient conditions for a stability and robustness.

After the discovery and analysis of the first two cones it was recognized that yet another cone was needed - this time with a dynamic radius. Such a cone was found by Thompson and reported in [6,7,8]. The result is shown below:

Lemma 5. Define the sampled-data operator $\tilde{K}$ and the LTI operators K and R. Assume that R^I is also a LTI operator, and that $\tilde{K}$, K, R and R^I are L_{2e}-stable. Then $\tilde{K}$ is strictly inside cone (K,R) if

$$\sigma_{min}[\underline{R}(j\omega)] \geq \frac{1}{(1-\varepsilon)^{1/2}} \left[\frac{1}{T^2} \sum_k \sum_{n\neq k} \sigma_{max}^2 \left(\underline{H}_k \underline{D}^* \underline{F}_n\right) + \sum_k \sigma_{max}^2 \left(\underline{H}_k \underline{D}^* \underline{F}_k - \underline{K}_k\right)\right]^{1/2}$$

for all ω and some $\varepsilon > 0$ (23)

Furthermore, the choice of center $\underline{K} = \frac{1}{T} \underline{H}\, \underline{D}^* \underline{F}$, called the "optimal center," minimizes the lower bound for the radius. ■

The proof is contained in the above references. The basic idea is to show that for all possible inputs the conic sector inequality (10) is satisfied. The summations and double summations in (23) result from the way the synchronous sampler shifts and adds the Laplace transform of the sampled input signal.

The size of the radius depends on how rapidly both the prefilter and the hold roll off. At one extreme both the prefilter and hold at band-limited, in which case (23) of Lemma 5 begins to look like (16) of Lemma 1. At the other extreme the prefilter or hold do not roll off, for example $\underline{F}(s)$ = constant, in which case the radius is infinite. As shown in [7], the infinite summations converge if both the prefilter and hold have at least a $\frac{1}{2}$ pole rolloff.

The size of the radius also depends on the choice of center. Poor choices result in large radii. An optimal choice is given in the statement of Lemma 5. It is optimal because it zeros out the single summation over k in (23). It has the potential disadvantage of being infinite dimensional, due to the e^{sT} terms. If needed, we didn't need it, a low order finite dimensional $\underline{K}(s)$ can be chosen, at the expense of a larger radius.

Approximate and exact methods for computing the radius are discussed in [7]. Because the radius is periodic and even it need only be computed for $0 \leq w \leq \frac{\pi}{T}$. The approximate analysis proceeds by truncating the infinite sums in (23) and showing that the remainder approaches zero. Usually[1] it suffices to truncate the single and double summations at ±20 terms. We found this to be the best way to compute the radius, and did so even for those cases where we know the exact solution.

The exact solution to (23) uses the matrix exponential. The most involved case we worked out is for a SISO $\tilde{K}$ when h(s) is a zero-order-hold and f(s) is given by a state space representation.[2]

[1] "Usually" means that the prefilter and hold have at least one pole rolloff with break frequencies < π/T rad/sec.

[2] We happened upon the following infinite series, which arises from the use of the zero-order-hold, and whose sum we haven't found in any tables:

$$\sum_k |h_k|^2 = 1, \text{ where } h(s) = (1-e^{-sT})/sT$$

IV. Stability and Robustness when $\tilde{K}$ is Strictly Inside of a Cone.

In this section we assume the existence of cones that respectively contain $\tilde{G}$ and $\tilde{K}$, and then we use their centers and radii to give sufficient conditions for closed loop stability. Because conic sectors are used this stability result is also a robustness result.

We must distinguish between the nominal and actual feedback systems. The usual procedure for analyzing robustness is to (1) define perturbations of the nominal system that include as a special case the actual system, (2) assume or show that the nominal system is closed loop stable, and (3) show that all allowable perturbations of the nominal system preserve the closed loop stability.

The nominal feedback system has the LTI loop transfer operator KG, and the actual feedback system has the LTV loop transfer operator $\tilde{K}\tilde{G}$. The closed loop stability result is now stated:

Theorem 1. The feedback system with the loop transfer operator $\tilde{K}G$ is closed loop stable if

(i) $\tilde{K}$ is strictly inside cone (K,R)

(ii) $G\ (I+KG)^{I}$ is L_{2e}-stable, i.e. the LTI nominal feedback system is closed loop stable (26)

(iii) $\sigma_{max}\ [\underline{R}\ \underline{G}\ (\underline{I} + \underline{KG})^{-1}(j\omega)] \leq 1$ for all ω

The actual feedback system with the loop transfer operator $\tilde{K}G$ is closed loop stable if in addition

(iv) $\ell_m(\omega) < \dfrac{\sigma_{min}[\underline{I} + \underline{K}\ \underline{G}(j\omega)] - \sigma_{max}[\underline{R}\ \underline{G}(j\omega)]}{\sigma_{max}[\underline{K}\ \underline{G}(j\omega)] + \sigma_{max}[\underline{R}\ \underline{G}(j\omega)]}$ for all ω ■ (27)

The first part of Theorem 1 determines closed loop stability for just the nominal plant. Condition (i) is that $\tilde{K}$ is strictly cone (K,R). If conditions (ii) and (iii) are true then by Lemma 2 it follows that $-G^{I}$ is outside of the same cone. Hence, by the conic sector stability condition (13), it follows that the feedback system with $\tilde{K}G$ is closed loop stable.

The second part of Theorem 1 determines closed loop stability for all allowable perturbations of the nominal plant characterized by $\ell_m(\omega)$. If condition (iv) is true then by Lemma 3 it follows that all allowable $\tilde{G}$'s satisfy the property that $-\tilde{G}^{I}$ is outside of cone (K,R_g). Hence, again by (13), it follows that the actual feedback system with $\tilde{K}\tilde{G}$ is closed loop stable.

One of the properties of an operator is its gain, as defined by (8). It is well known, at least to those that already know it, that the gain of a LTI operator G is

$$\| G \| = \sup_{0<\omega<\infty} \sigma_{max}[\underline{G}(j\omega)] \tag{24}$$

As a corollary to Lemma 5, we can find an upperbound for the gain of a sampled-data operator $\tilde{K}$. For the SISO case we can construct a signal that achieves the upperbound, see [7] and [8], thereby showing that the upperbound actually is the gain.

Lemma 6. An upperbound for the gain of the sampled-data operator $\tilde{K}$ is

$$\| \tilde{K} \| \leq \sup_{0\leq\omega\leq\frac{\pi}{T}} \left[\frac{1}{T^2} \sum_k \sum_n \sigma_{max}^2 (\underline{H}_k \underline{D}^* \underline{F}_n) \right]^{1/2} \tag{25}$$

Furthermore, this upperbound equals the gain when $\underline{H}$, $\underline{D}^*$, and $\underline{F}$ are SISO. ■

This result is proved in a few steps by substituting the zero center $\underline{K}(s) = 0$ into (23) of Lemma 5 and then by taking the suprenum over the fundamental frequency range. We have not yet succeeded in constructing a signal which achieves the upperbound for the multivariable case, and conjecture that (25) actually is the gain. The algebra is considerably more complex than for the SISO case, where it is bad enough, and we leave the multivariable result as an incentive for someone else to become interested in this problem.

At this point we have established the fundamental result, Lemma 5, which shows the existence of a cone that contains a sampled-data operator. The key fact that distinguishes this cone from earlier ones is that its radius is dynamic (i.e. has a nonconstant Laplace transform). We now proceed to demonstrate its usefulness.

To apply Theorem 1 start with a description of a sampled-data control system, i.e. knowledge of $\underline{F}(s)$, T, $\underline{D}(z)$, $\underline{H}(s)$, $\underline{G}(s)$, and $\ell_m(\omega)$. Construct a cone that contains K by choosing a center and then by computing the radius using (23) of Lemma 5. Check condition (ii) of Theorem 1 by any of a variety of techniques for determining closed loop stability of LTI systems. Graphically check conditions (iii) and (iv) to determine closed loop stability of the actual system.

Example 1. In this example Theorem 1 is demonstrated. We start with the SISO control system with the LTI plant and compensator:

$$g(s) = \frac{150}{(s+1)(s+3)} \tag{28a}$$

$$k_a(s) = \frac{(s+3)^2}{(s+.4)(s+22.5)} \tag{28b}$$

The compensator was designed by classical control techniques (loop shaping on a Bode plot) so as to meet the specifications (i) dc gain $\geq$ 50, (2) phase margin > 45°, and (3) bandwidth < 12 rad/sec. The lead-lag compensator contributes phase lag below 3 rad/sec and phase lead above 3 rad/sec. The phase margin is about 60°, which was set high to account for the inevitable phase lag introduced by a sampled-data compensator.

The LTI compensator is to be digitally implemented. The following are chosen for the prefilter, sample period, digital computer z-transform, and hold:

$$f(s) = \frac{2500}{s^2+70s+2500} \text{ (2nd order Butterworth, break freq = 50 rad/sec)} \tag{29a}$$

$$T = .031416 \text{ sec (foldover freq = 100 rad/sec)} \tag{29b}$$

$$d(z) = \frac{.80498(z-.90993)^2}{(z-.98750)(z-.47744)} \text{ (Tustin prewarped about 3 rad/sec)} \tag{29c}$$

$$h(s) = \frac{1-e^{-sT}}{s} \text{ (zero-order-hold)} \tag{29d}$$

The conic sector analysis techniques do not depend on any particular method for designing the sampled-data compensator. We have chosen to discretize an analog compensator. Another possibility is to first discretize the plant and then design d(z) by a direct digital method.

A cone is now constructed that contains the sampled-data operator. The optimal center is chosen and the radius is computed by truncating (23):

$$k(j\omega) = \frac{1}{T} h\, d^*\, f \tag{30a}$$

(30)

$$r(j\omega) = \frac{1}{T}\left[\sum_{k=20}^{20} \sum_{\substack{n=-20 \\ n\neq k}}^{20} |h_k d^* f_n|^2\right]^{1/2} \text{ for } 0 \leq \omega \leq \frac{\pi}{T}$$

A magnitude Bode plot of the radius $r(j\omega)$ is shown in Figure 3. The multiplicative radius $k^{-1}r(j\omega)$ and the loop transfer function $kg(j\omega)$ of the nominal system are shown in Figure 4.

The multiplicative radius gives the relative size of the center and radius and is more useful than the absolute size of the radius. As seen in Figure 4 the multiplicative radius is << 1 at low frequencies, indicating that the center is a good approximation of the sampled-data operator. At frequencies where the multiplicative radius is slightly less than or greater than 1 the center is a poor approximation of the sampled-data operator. At these frequencies the loop gain should be << 1, as is the case in Figure 4.

The cone we just constructed satisfies condition (i) of Theorem 2. Condition (ii) is that the nominal feedback system with the loop transfer function $kg(j\omega)$ is closed loop stable. That it is indeed closed loop stable can be shown by a straightforward use of Bode, Nyquist, or Nichols plots. Because $k(j\omega)$ is infinite dimensional it is not feasible to examine closed loop pole locations.

Condition (iii) of Theorem 1 is verified in Figure 5, where it is shown that

$$| rg(1+gk)^{-1}(j\omega) | < 1 \text{ for all } \omega \tag{31}$$

At this point we know that the sampled-data control system is closed loop stable for the nominal plant.

Condition (iv) is satisfied for any $\ell_m(\omega)$ such that

$$\ell_m(\omega) < \frac{| 1+kg | - | rg |}{| kg | + | rg |} \text{ for all } \omega \tag{32}$$

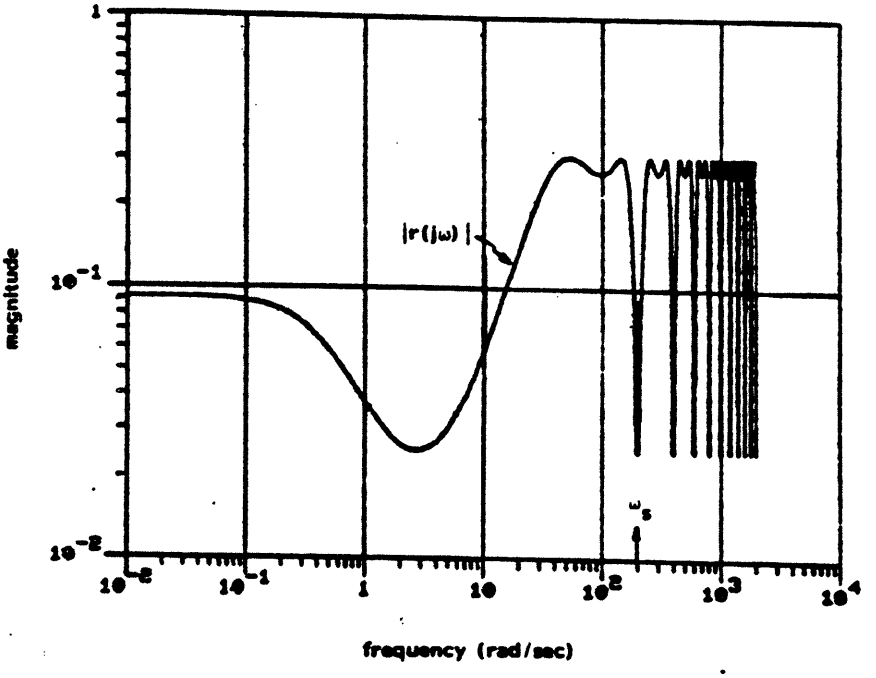

Figure 3: The radius $r(j\omega)$ of the cone that contains $\tilde{K}$ of example 1

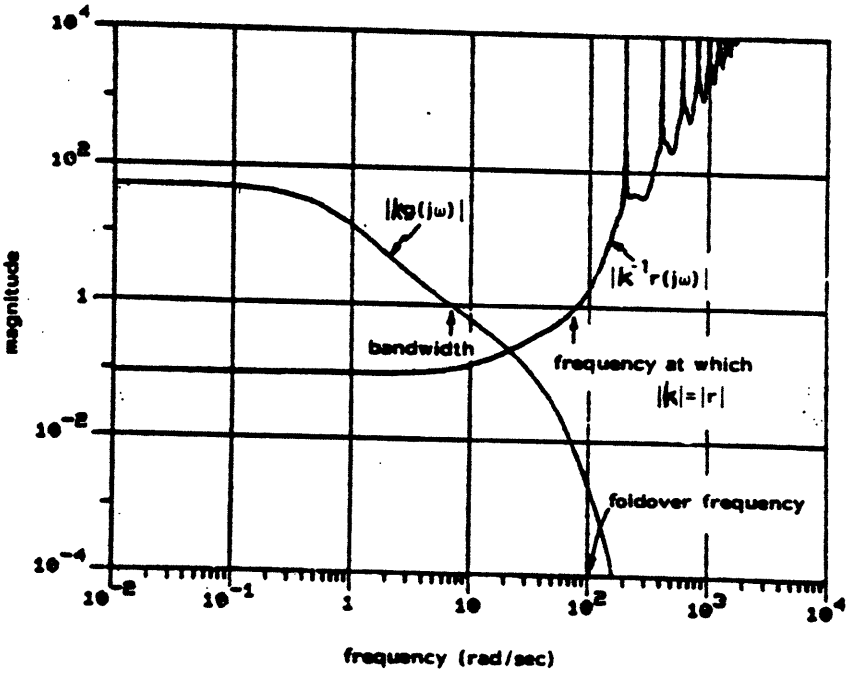

Figure 4: The multiplicative radius $k^{-1}r(j\omega)$ and the loop transfer function $kg(j\omega)$

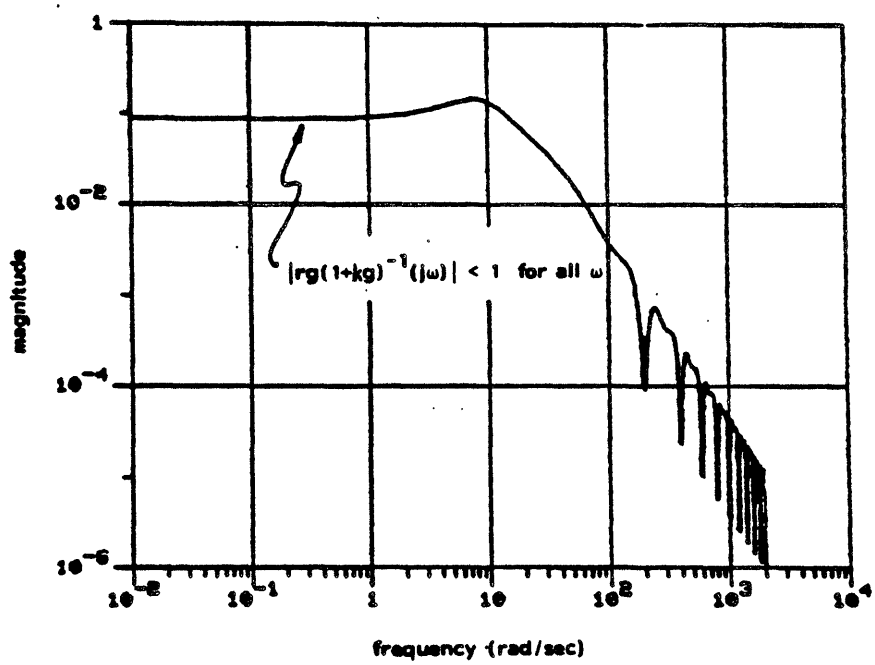

Figure 5: Condition (iii) of Theorem 1, tested for example 1

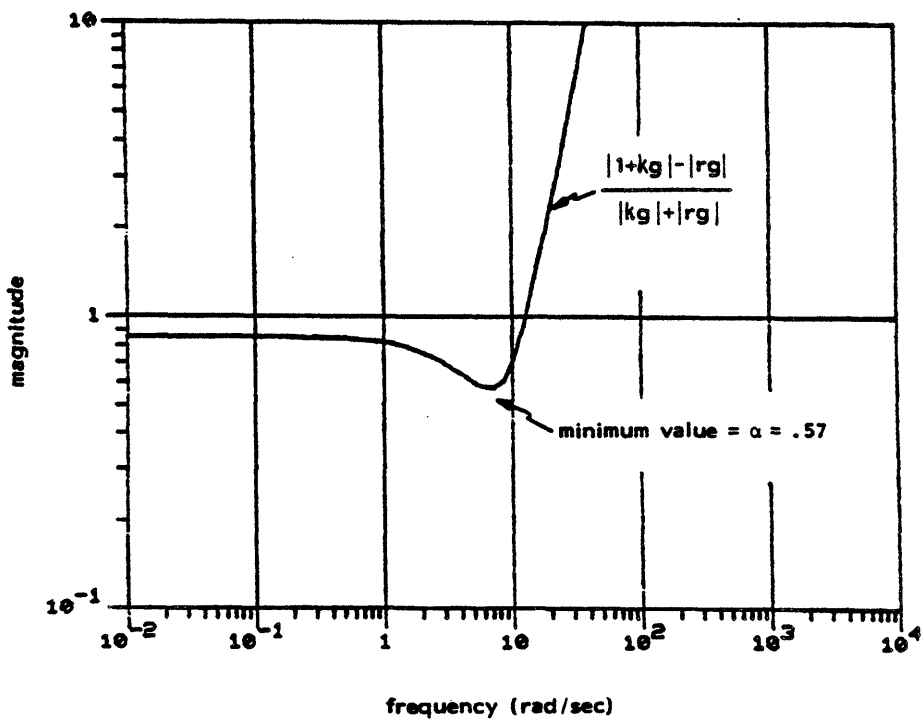

Figure 6: Condition (iv) of Theorem 1, tested for example 1

The right hand side of (32) is plotted in Figure 6. Various types of $\ell_m(\omega)$'s can be concocted to correspond to uncertainties in $g(j\omega)$, such as phase uncertainties, gain uncertainties, unmodelled higher order dynamics, unmodelled time delays, and so on. For example, the minimum value of $\alpha = .57$ in Figure 6 guarantees that the closed loop system will remain stable in spite of phase uncertainties in $g(j\omega)$ up to $\pm\cos(1-\alpha^2/2) = \pm 33°$ at all frequencies [13]. Theorem 1 only gives sufficient conditions for closed loop stability, which means that a $\ell_m(\omega)$ that violates (32) may still result in a closed loop stable system.

This completes the section on analyzing stability and robustness when $\tilde{K}$ and $\tilde{G}$ are each strictly inside their respective cones. The next section is a variation on this theme, which involves splitting up the loop transfer operator into two different operators $\tilde{T}$ and $\tilde{I}$ and placing each of these strictly inside their respective cones.

V. Stability and Robustness when $\tilde{T}$ is strictly Inside of a Cone

In some cases it is better to combine the nominal plant G with the compensator $\tilde{K}$ and place the combination strictly inside of a cone. We have seen in the previous section that the size of the radius depends on the amount of rolloff of both the prefilter and hold. The intuitive idea used in this section is that the rolloff of the plant can be used to increase the rolloff of the prefilter and/or hold.

The question arises where to place the plant? For the purpose of analysis we can break the feedback loop anywhere we want, which determines where the plant is placed. Define $\tilde{T}$ as the combination of $\tilde{K}$ and G. Both $\tilde{K}$ and $\tilde{T}$ are sampled-data operators. Associated with $\tilde{K}$ are $\underline{F}(s)$, T, $\underline{D}(z)$, and $\underline{H}(s)$. Associated with $\tilde{T}$ are $\tilde{\underline{F}}(s)$, T, $\underline{D}(z)$, and $\tilde{\underline{H}}(s)$. Where the loop is broken determines $\tilde{\underline{F}}(s)$ and $\tilde{\underline{H}}(s)$. Always it must be the case that $\tilde{\underline{F}}\tilde{\underline{H}}(s) = \underline{FGH}(s)$. Three choices are

$$\text{Plant with hold:} \quad \tilde{\underline{F}} = \underline{F} \quad , \quad \tilde{\underline{H}} = \underline{G}\,\underline{H}$$

$$\text{Plant with prefilter:} \quad \tilde{\underline{F}} = \underline{F}\,\underline{G} \quad , \quad \tilde{\underline{H}} = \underline{H}$$

$$\text{Optimal combination:} \quad \tilde{\underline{F}} = (\underline{F}\,\underline{G}\,\underline{H})^{1/2}, \quad \tilde{\underline{H}} = (\underline{F}\,\underline{G}\,\underline{H})^{1/2}$$

Deciding how to combine the nominal plant and the sampled-data operator adds a layer of difficulty to the conic sector analysis. This difficulty can be resolved for the SISO case. Assume a cone (T, R_t) is constructed that contains $\tilde{T}$. The radius $r_t(j\omega)$ is minimized for each ω by the optimal combination of $\tilde{G}$ and K shown in (33). This is proved in Appendix B. The importance of this result is that it gives the least conservative sufficient conditions for closed loop stability and robustness. A block diagram of the sampled-data feedback system showing the optimal combination of G and $\tilde{K}$ is in Figure 7.

For any combination of G and $\tilde{K}$ the end result is that the sampled-data feedback system is divided into two elements $\tilde{T}$ and $\tilde{I}$. The LTI operator $\tilde{I}$ is the perturbation of the plant. It is strictly inside of a cone with the identity operator I as the center and a radius determined by $\ell_m(\omega)$. The nominal feedback system has the LTI loop transfer operator T, and the actual feedback system has the LTV loop transfer operator $\tilde{T}\tilde{I}$. Sufficient conditions for the actual feedback system to be closed loop stable are given in Theorem 2, which is a variation of Theorem 1.

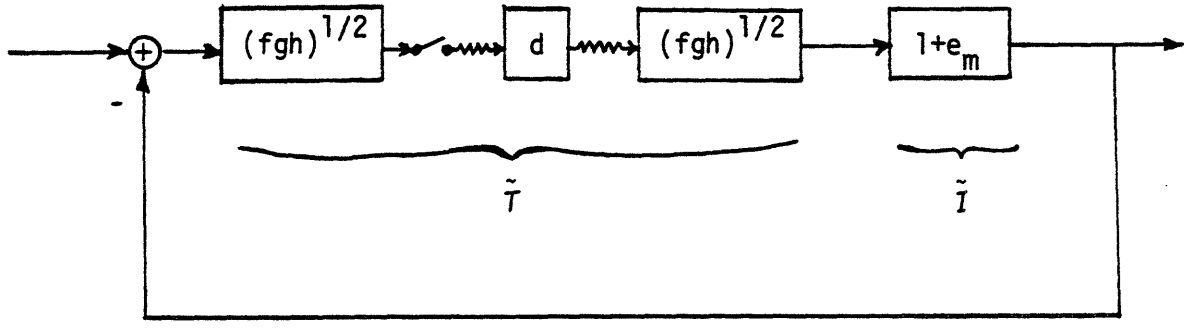

Figure 7: The optimal $\tilde{T}$ for SISO systems

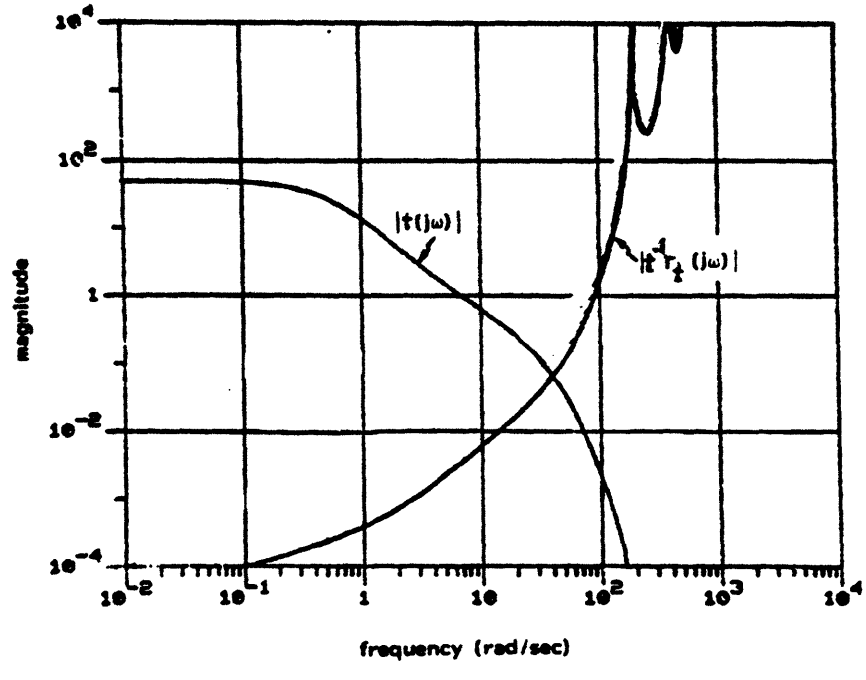

Figure 8: The multiplicative radius $t^{-1}r_t(j\omega)$ and the loop transfer function $t(j\omega)$ for example 2

Theorem 2. The feedback system with the loop transfer operator $\tilde{T}$ is closed loop stable if

(i) $\tilde{T}$ is strictly inside cone (T,R_t)

(ii) $(I+T)^I$ is L_{2e}-stable, i.e. the LTI nominal feedback system is closed loop stable

(iii) $\sigma_{max}\,[\underline{R}_t(\underline{I}+\underline{T})^{-1}(j\omega)] \leq 1$ for all ω (34)

The actual feedback system with the loop transfer operator $\tilde{T}$ is closed loop stable if in addition

(iv) $$\ell_m(\omega) < \frac{\sigma_{min}[\underline{I}+\underline{T}(j\omega)]-\sigma_{max}[\underline{R}_t(j\omega)]}{\sigma_{max}[\underline{T}(j\omega)]+\sigma_{max}[\underline{R}_t(j\omega)]} \qquad \blacksquare \qquad (35)$$

The proof of Theorem 2 is similar to the proof of Theorem 1. If the first three conditions are true then $\tilde{T}$ is strictly inside and $-I$ is outside cone (T,R_t). If in addition condition (iv) is true then all allowable $\tilde{I}$'s satisfy the property that $-\tilde{I}^I$ is outside cone (T,R_t).

Example 2. We start with the same analog system (28) and sampled-data compensator (29) as in Example 1. In this example we choose $\tilde{T}$ to be the optimal combination of G and K, construct a cone (T,R_t) that contains $\tilde{T}$, and then use Theorem 2 to determine close loop stability. We will see that the optimal combination of G and $\tilde{K}$ results in less conservative robustness margins than in Example 1. This example then continues by showing how the radius depends on the choice of the sample rate.

The optimal combination $\tilde{T}$ of G and $\tilde{K}$ is shown in Figure 7. We now construct a cone (T,R_t) that contains this $\tilde{T}$. The optimal center is chosen and the radius is computed by truncating (23) of Lemma 5:

$$t(jw) = \frac{1}{T}\, ghd^* f \qquad (36a)$$

$$r_t(j\omega) = \frac{1}{T}\left[\sum_{k=-20}^{20}\ \sum_{\substack{n=-20 \\ n\neq k}}^{20} |(fgh)_k d^* (fgh)_n|\right]^{1/2} \quad \text{for } 0 \leq \omega \leq \frac{\pi}{T} \qquad (36b)$$

We know that this radius is smaller at each ω than for any other combination of G and $\tilde{K}$. The magnitude Bode plot of the center $t(j\omega)$ and the multiplicative radius $t^{-1}r_t(j\omega)$ are shown in Figure 8.

We now check the conditions of Theorem 2. Condition (i) is satisfied by the cone just constructed. Condition (ii) is satisfied because the nominal LTI feedback system is the same as in Example 1, and we already know it is closed loop stable. Condition (iii) is verified in Figure 9, where it is shown that

$$| r_t(1+t)^{-1}(j\omega) | \leq 1 \text{ for all } \omega \tag{37}$$

At this point we know the sampled-data system with the nominal plant is closed loop stable. Stability is preserved for any multiplicative perturbation of the nominal plant that satisfies condition (iv), which is

$$\ell_m(\omega) < \frac{| 1+t(j\omega) | - | r_t(j\omega) |}{| t(j\omega) | + | r_t(j\omega) |} \text{ for all } \omega \tag{38}$$

The right hand side of (38) is shown in Figure 10. Its minimum value of $\alpha = .74$ guarantees that stability is preserved for phase uncertainties in $g(j\ )$ up to $\pm 43°$ at all frequencies. By placing $\tilde{T}$ and not just $\tilde{K}$ strictly inside of a cone we have obtained a less conservative robustness margin. It comes close to meeting our original specification of a 45° phase margin.

Selecting the Sample Period. We continue Example 2 by demonstrating how conic sector techniques can be used to select the sample period T. Both the center and the radius of the cone (T, R_t) depend on T. Here we choose T so that the multiplicative radius is much less than one ($t^{-1}r_t << 1$) over the bandwidth of the nominal LTI system ($t > 1$).

All of the components of the sampled-data compensator depend on T. Here we select these components so that T is the only variable:

$$f(s) = \text{2nd order Butterworth with break freq} = \frac{\pi}{2T} \text{ rad/sec} \tag{39a}$$

$$d(z) = \text{Tustin prewarped version of } k_a(s) \text{ about 3 rad/sec} \tag{39b}$$

$$h(s) = \text{zero-order-hold} \tag{39c}$$

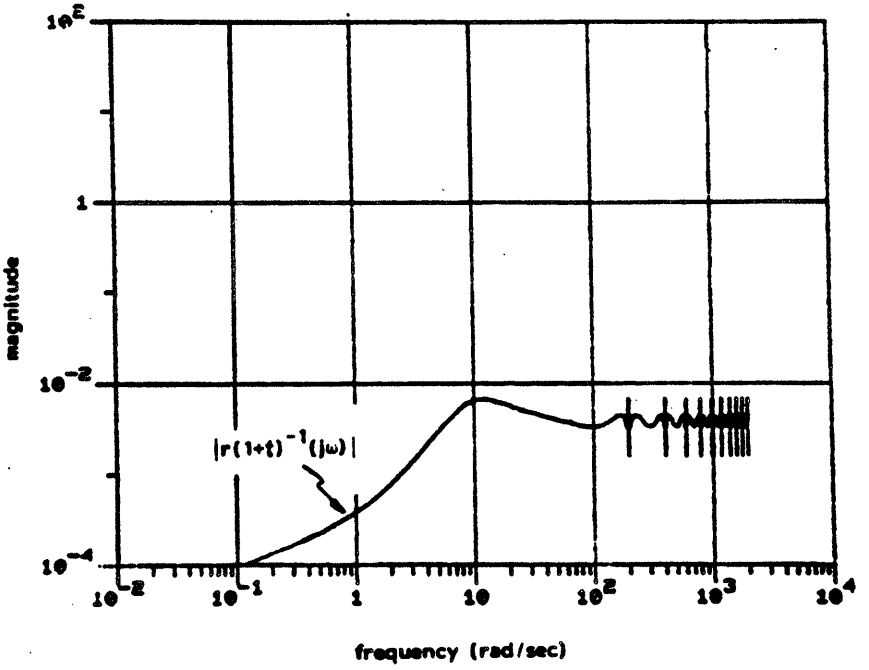

Figure 9: Condition (iii) of Theorem 2, tested for example 2

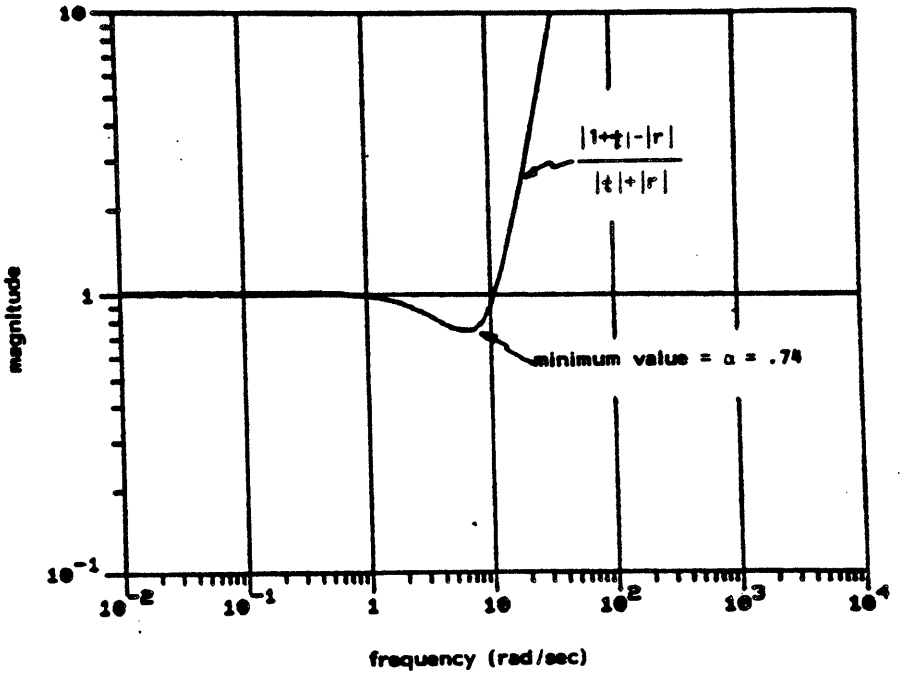

Figure 10: Condition (iv) of Theorem 2, tested for example 2

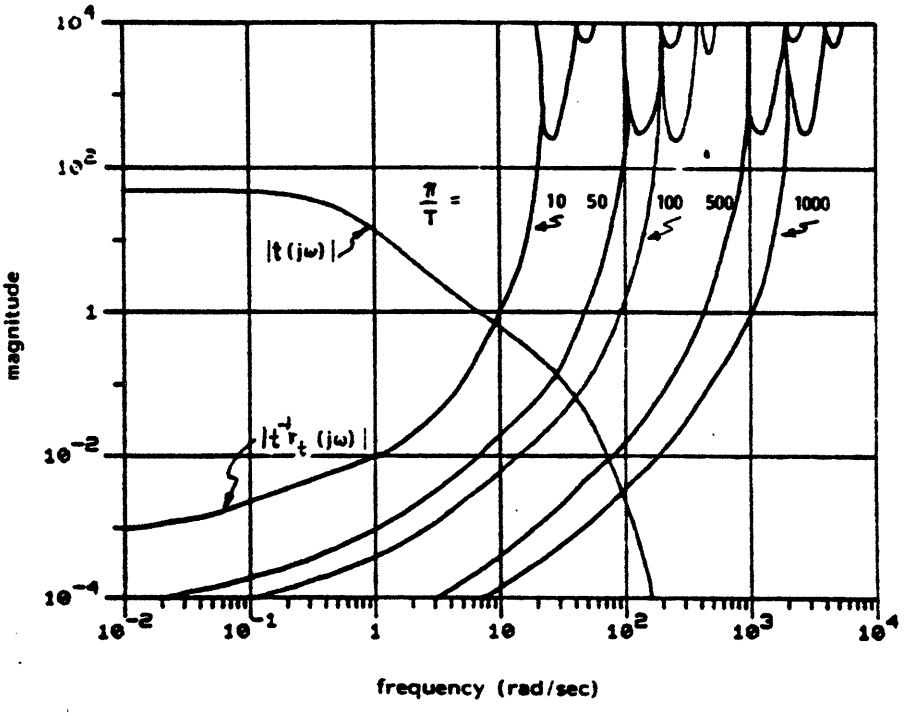

Figure 11: Multiplicative radii $t^{-1}r(j\omega)$ used to select sample rate

For each of five sample periods a cone (T,R_t) is constructed around $\tilde{T}$. The optimal combination of G and $\tilde{K}$ is used for $\tilde{T}$, which means that the prefilter and hold of $\tilde{T}$ are each $(fgh)^{1/2}$. The five sample periods are T = .31416, .062832, .031416, .002832, and .0031416 seconds; which correspond respectively to the foldover frequencies π/T = 10, 50, 100, 500, and 1000 rad/sec. The multiplicative radii are shown in Figure 11 and compared with the center of the cone when the sample period is the T = .031416 used earlier in this example.

The multiplicative radius is a frequency dependent modelling error and it behaves as we intuitively expect it to - as the sample period T decreases the frequency range increases over which the modelling error is significant. We see from Figure 11 that there is little to be gained by decreasing T below .031416 seconds, because the multiplicative radius is already << 1 over the bandwidth of the system. Also we must consider that the plant has its own frequency dependent modelling error $\ell_m(\omega)$ and there is little to be gained by decreasing the multiplicative radius so that $t^{-1}r << \ell_m$.

On the other hand, we see from Figure 11 that increasing T to .31416 seconds increases the size of the multiplicative radius so that it is significant near the bandwidth of 7 rad/sec. This indicates trouble with either stability or poor robustness margins.

This completes the section of placing $\tilde{T}$ and $\tilde{I}$ strictly inside of their respective cones. Now we move on to what might be considered the opposite approach.

VI. Stability and Robustness when $-\tilde{K}^I$ is Outside of a Cone.

The conic sector analysis techniques of Sections IV and V respectively place $\tilde{K}$ and $\tilde{T}$ strictly inside of cones. These techniques differ in how the nominal plant G is treated, but both work by placing the sampled-data portion of the loop transfer operator $\tilde{G}\,\tilde{K}$ strictly strictly inside of a cone. The major restriction to these techniques, you may have noticed, is that the sampled-data operators $\tilde{K}$ and $\tilde{T}$ must be open-loop stable.

In this section we change the analysis techniques so that the sampled-data portion of $\tilde{G}\,\tilde{K}$ is outside of a cone. We do so by constructing a cone (G,R_g) such that $-\tilde{K}^I$ is outside of the cone. This is possible if the nominal feedback system with the loop transfer operator $G\,\tilde{K}$ is closed loop stable, as can be determined by digital techniques (discrete Nyquist, location of plane poles, guaranteed stability by discrete optimal control, and so on). This condition is less restrictive than open loop stability of $\tilde{K}$ or $\tilde{T}$.

Note that we have changed the nominal system from the $G\,K$ of the previous two sections to the $G\,\tilde{K}$ of this section. We lose the intuitive appeal of a LTI nominal system, but gain by having a less restrictive analysis technique. No matter what choice is for a nominal system, the actual system will always have the loop transfer function $G\,\tilde{K}$.

In the following Lemma sufficient conditions are given for the existence of a cone such that $-\tilde{K}^I$ is outside of the cone.

Lemma 7. Define the sampled-data operator $\tilde{K}$ and the LTI operators G and R_g. Assume that R_g^I and $(I + G\,\tilde{K})^I$ are also LTI operators, and that both R_g and R_g^I are L_{2e}-stable. Then $-\tilde{K}^I$ is outside cone (G,R_g) if

(i) $\tilde{K}\,(I + G\,\tilde{K})^I$ is L_{2e}-stable

(ii) $$\sigma_{max}[\underline{R}_g(j\omega)] \leq \left[\frac{1}{T^2}\sum_k\sum_n \sigma_{max}^2\,(\underline{H}_k\underline{D}^*_{c\ell}\underline{F}_n)\right]^{1/2} \quad \text{for all } \omega \quad \blacksquare \quad (40)$$

The proof of Lemma 7 is contained in [7] and [8]. The proof is similar to that of Lemma 5, due to the fact that $\tilde{K}\,(I + G\,\tilde{K})^I$ is a sampled-data operator with a structure similar to $\tilde{K}$. They have the same prefilters, sample periods, and hold devices; and differ in that $\tilde{K}$ has the digital computer $\underline{D}(z)$ as opposed to $\underline{D}_{c\ell}(z)$ of (5). Lemma 5 is true, i.e. $\tilde{K}$ is strictly inside cone (K,R), if and only if the composite operator $(\tilde{K}-K)R^I$ has gain < 1. Lemma 7

is true, i.e. $-\tilde{K}^I$ is outside cone (G,R_g), if and only if the composite operator $R_g\tilde{K}\ (I + G\ \tilde{K})^I$ has gain < 1. The proofs of Lemmas 5 and 7 use similar methods to show the gains are < 1.

Sufficient conditions for closed loop stability are given below in Theorem 3. If conditions (i) and (ii) are true then $-\tilde{K}^I$ is outside cone (G,R_g), and if condition (iii) is true then $\tilde{G}$ is strictly inside of the same cone. Hence, by (14), the closed loop system is stable. The following theorem is a robustness as well as a stability result, because it applies to any $\tilde{G}^I$ strictly inside of cone (G,R_g).

Theorem 3. The actual feedback system with the loop transfer operator $\tilde{G}\ \tilde{K}$ is closed loop stable if

(i) $\tilde{K}\ (I + G\ \tilde{K})^I$ is L_{2e}-stable, i.e. the nominal feedback system with the loop transfer operator $G\ \tilde{K}$ is closed loop stable

(ii) $-\tilde{K}^I$ is outside cone (G,R_g)

(iii) $\ell_m(\omega) < \sigma_{min}[R_g(j\omega)]/\sigma_{max}[\underline{G}(j\omega)]$ for all ω (41)

This theorem is implemented in three steps. First, the closed loop stability of the nominal feedback system is determined by digital techniques. Second, the radius $\underline{R}_g(j\omega)$ is computed by equation (40) of Lemma 7. Third, the inequality (41) is graphically checked.

Example 3. The conic sector analysis technique of Theorem 3 is demonstrated for a SISO example. The open loop plant and prefilter are

$$g(s) = \frac{1}{s+1} \tag{42a}$$

$$k_a(s) = \frac{1}{s} \tag{42b}$$

Due to the analog integrator the closed loop system has zero steady state error for a step input. The closed loop bandwidth is .8 rad/sec. The sampled-data implementation of the analog integrator is:

$$f(s) = \frac{25}{s^2+70s+25} \quad \text{(2nd order Butterworth with break freq = 5 rad/sec)} \tag{43a}$$

$$T = .31416 \text{ seconds (foldover freq = 10 rad/sec)} \tag{43b}$$

$$d(z) = .1579\,\frac{z+1}{z-1} \quad \text{(Tustin prewarped about .8 rad/sec)} \tag{43c}$$

$$h(s) = \text{zero-order hold} \tag{43d}$$

Though this example is very simple it serves the purpose of demonstrating Theorem 3 for systems with digitally implemented integrators.

The first step in implementing Theorem 3 is to show that the nominal closed loop system is closed loop stable. This can be done, for example, by plotting the discrete Nyquist diagram $d(z)g_d(z)$ for $z = e^{j\omega T}$ and $0 \leq \omega \leq \pi/T$. The second step is to compute $r_g(j\omega)$ by truncating (40):

$$r_g(j\omega) = \left[\frac{1}{T^2}\sum_{k=-20}^{20}\sum_{n=-20}^{20} | h_k d^*_{c\ell} f_n |\right]^{1/2} \qquad \text{for } 0 \leq \omega \leq \frac{\pi}{T} \tag{44}$$

Stability of the actual feedback system is preserved for any multiplicative perturbation $\ell_m(\omega)$ that satisfies

$$\ell_m(\omega) < | r_g(j\omega)/g(j\omega) | \quad \text{for all } \omega \tag{45}$$

The right hand side of (45) is shown in Figure 12. As mentioned earlier, many different $\ell_m(\omega)$'s can be concocted to correspond to a variety of plant uncertainties. The minimum value of $\alpha = .53$ in Figure 11 corresponds to a tolerance for ±31° phase uncertainty in $g(j\omega)$ at all frequencies.

This completes the section on placing $-\tilde{K}^I$ outside of a cone, which is the last of the three conic sector analysis techniques presented in this paper.

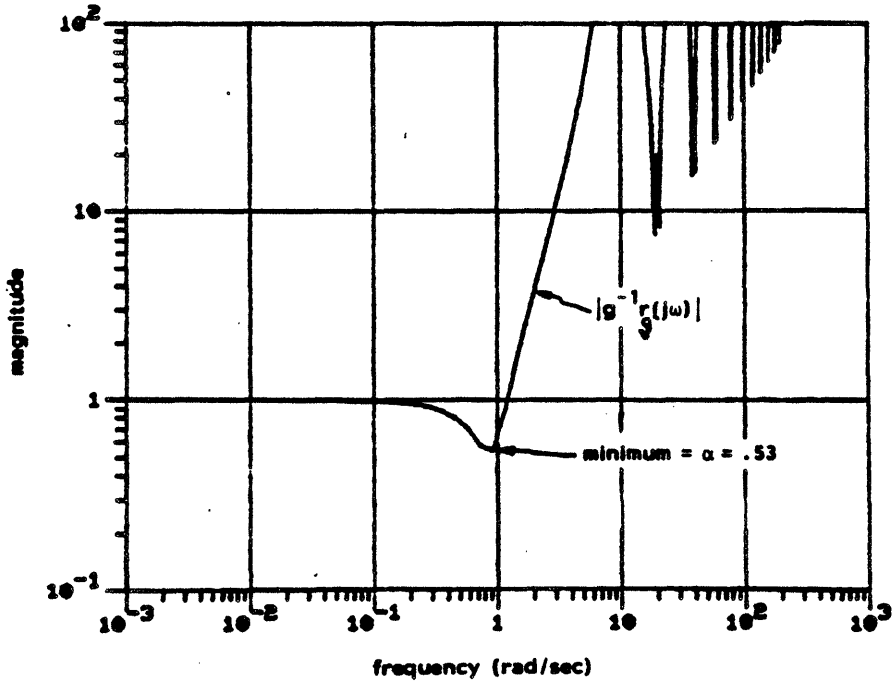

Figure 12: Condition (iii) of Theorem 3, tested for example 3

VII. Conclusion.

Conic sectors can be used to determine closed loop stability and to analyze robustness of sampled-data feedback systems. Analysis techniques based on conic sectors form an alternative to the use of z-transforms. They have a practical advantage in that the robustness margins depend on the prefilter, sample period, and hold device; and therefore can be used to help in their selection. Conic sector analysis techniques also have a conceptual advantage in that they allow the sampled-data feedback system to be rigorously approximated by a LTI feedback system. Frequency dependent modelling errors are due to (1) the plant uncertainties and (2) the use of a sampled-data as opposed to a LTI compensator.

In Sections II and III of this paper some background material was reviewed leading up to a new conic sector (Lemma 5), which is considered "useful" because it is computable and results in nonconservative sufficient conditions for stability and robustness. We do not focus attention on mathematical proofs, most of which are referenced, but on the following analysis techniques, which differ in how the loop transfer operator is divided:

Section IV: $\tilde{K}$ is strictly inside and $-\tilde{G}^I$ is outside cone (K,R)

Section V: $\tilde{T}$ is strictly inside and $-\tilde{I}^I$ is outside cone (T,R_t)

Section VI; $\tilde{G}$ is strictly inside and $-\tilde{K}^I$ is outside cone (G,Rg)

Equations are given to construct each of these cones. Their centers and radii are then used to graphically determine closed loop stability and robustness margins.

The research to date has concentrated on the use of conic sectors to analyze sampled-data feedback systems with single synchronous samplers. This is a class of systems for which z-transform techniques work well, albeit with a few loose ends concerning the selection of prefilters and sample rates.

Further research is being conducted to extend these results to systems with nonsynchronous samplers or with multiple samplers operating at different rates. Existing z-transform techniques work less well for these systems, and it is here that conic sector analysis techniques may prove to be the most beneficial. Preliminary results for the multirate case [7] have already been obtained.

Appendix A

Proof of Lemma 3

The objective is to show that all $\tilde{G}$'s strictly inside cone (G,R_g) are outside cone (K,R). This is done by showing that all such $\tilde{G}$'s satisfy conditions (i) and (ii) of Lemma 2.

Condition (i) is that $\tilde{G}\ (I + K\ \tilde{G})^I$ is L_{2e}-stable. It is assumed that $G\ (I + K\ G)^I$ is L_{2e}-stable, and it is a LTI robustness result, e.g. [12], that $\tilde{G}\ (I + K\ \tilde{G})^I$ is L_{2e}-stable if

$$\ell_m(\omega) < \frac{\sigma_{min}[\underline{I} + \underline{K}\ \underline{G}\ (j\omega)]}{\sigma_{max}[\underline{K}\ \underline{G}\ (j\omega)]} \quad \text{for all } \omega \tag{A.1}$$

which is implied by (19) of Lemma 3.

Condition (ii) of Lemma 2 is true for all allowable $\tilde{G}$'s because:

$$\sigma_{max}[\underline{R}\ \tilde{\underline{G}}\ (\underline{I} + \underline{K}\ \tilde{\underline{G}})^{-1}(j\omega)] \leq \sigma_{max}[\underline{R}\ \tilde{\underline{G}}]/\sigma_{min}[\underline{I} + \underline{K}\ \tilde{\underline{G}}] \tag{A.2}$$

$$\leq \sigma_{max}[\underline{R}\ \underline{G}](1+\ell_m)/\sigma_{min}[\underline{I} + \underline{K}\ \tilde{\underline{G}}] \tag{A.3}$$

$$\leq \sigma_{max}[\underline{R}\ \underline{G}](1+\ell_m)/\{\sigma_{min}[\underline{I} + \underline{K}\ \underline{G}] - \sigma_{max}[\underline{K}\ \underline{G}]\ \ell_m\} \tag{A.4}$$

$$\leq 1 \tag{A.5}$$

The last step is implied by (19) of Lemma 3, and this completes the proof.

Appendix B

The Optimal Combination of $\tilde{K}$ and G.

The sampled-data operator $\tilde{K}$ and nominal plant G can be combined in many different ways, each resulting in a different $\tilde{T}$. Here we show SISO systems that the $\tilde{T}$ of Figure 6 minimizes the radius of the cone (T,R_t).

The prefilter, digital computer, and hold devide for $\tilde{T}$ are respectively $\tilde{f}(s)$, $d(z)$, and $\tilde{h}(s)$. It must always be the case that $\tilde{h}\tilde{f} = fgh$. For any choice of $\tilde{h}$ and $\tilde{f}$ assume the center of the cone is the same. The radius is:

$$r_t(j\omega) = [r_1(\omega) + r_2(\omega) + r_3(\omega)]^{1/2}, \text{ where} \tag{B.1a}$$

$$r_1(\omega) = \frac{1}{T^2} | d^* |^2 [\sum_k | \tilde{h}_k |^2][\sum_n | \tilde{f}_n |^2] \tag{B.1b}$$

$$r_2(\omega) = \frac{1}{T^2} | d^* |^2 [\sum_k | \tilde{h}_k \tilde{f}_k |^2] \tag{B.1c}$$

$$r_3(\omega) = \sum_k | \frac{1}{T^2} \tilde{h}_k d^* \tilde{f}_k - t_k | \tag{B.1d}$$

Equation (B.1) follows in a few steps from (23) of Lemma 5. The double summation in (23) is converted to a single summation by adding and subtracting the k = n term.

The only part of the radius calculation that depends on the particular choice of $\tilde{f}$ and $\tilde{h}$ is the $r_2(\omega)$ term. We know from the Cauchy-Schwartz inequality that

$$[\sum_k | \tilde{h}_k \tilde{f}_k |]^2 \leq [\sum_k | \tilde{h}_k |^2] [\sum_n | \tilde{f}_n |^2] \tag{B.2}$$

Hence, $r_1(\omega)$ is minimized for each ω when $\tilde{h} = \tilde{f}$, which means that $r_t(\omega)$ is minimized for each ω when both $\tilde{h}$ and $\tilde{f}$ are equal to $(fgh)^{1/2}$.

References

[1] G. F. Franklin and J. D. Powell, Digital Control of Dynamic Systems, Addison-Wesley Publishing Co., Reading, MA, 1980.

[2] G. Zames, "On the Input-Output Stability of Time-Varying Nonlinear Feedback Systems, Parts I and II," IEEE Trans. Auto. Control, Vol. AC-11, pp. 228-238, April, 1966, and pp. 465-476, July, 1966.

[3] M. G. Safonov, Stability and Robustness of Multivariable Feedback Systems, The MIT Press, Cambridge, MA, 1980.

[4] M. G. Safonov and M. Athans, "A Multiloop Generalization of the Circle Criterion for Stability Margin Analysis," IEEE Trans. Auto. Control, Vol. AC-26, pp. 415-422, April, 1981.

[5] A. Kostovetsky, "Some Investigations of Hybrid Systems," S.M. Thesis, Dept. of Mech. Engr., MIT, May 1980, Appendix to Lab. for Info. and Dec. Systems Report LIDS-FR-960.

[6] G. Stein, M. Athans, and P. M. Thompson, "Hybrid Operator Models for Digitally Implemented Control Systems," Final Report for NASA Langley Research Center, NASA Grant No. NAG1-2, MIT Lab. for Info. and Dec. Systems Report LIOS-FR-1206, April, 1982.

[7] P. M. Thompson, "Conic Sector Analysis of Hybrid Control Systems," Ph.D. Thesis, MIT Lab. for Info. and Dec. Systems Report LIDS-TH-1242, September, 1982.

[8] P. M. Thompson, G. Stein, and M. Athans, "Conic Sectors for Sampled-Data Feedback Systems," submitted to Systems and Control Letters.

[9] M. G. Safonov, A. J. Laub, and G. L. Hartmann, "Feedback Properties of Multivariable Systems: The Role and Use of the Return Difference Matrix," IEEE Trans. Auto. Control, Vol. AC-26, pp. 47-65, February, 1981.

[10] V. C. Klema and A. J. Laub, "The Singular Value Decomposition: Its Computation and Some Applications," IEEE Trans. Auto. Control, Vol. AC-25, pp. 164-176, April, 1980.

[11] J. C. Willems, The Analysis of Feedback Systems, The MIT Press, Cambridge, MA, 1971.

[12] J. C. Doyle and G. Stein, "Multivariable Feedback Design: Concepts for a Classical/Modern Synthesis," IEEE Trans. Auto. Control, Vol. AC-26, pp. 4-16, February, 1981.

[13] N. A. Lehtomaki, N. R. Sandell, Jr., and M. Athans, "Robustness Results in Linear-Quadratic Guassian Based Multivariable Control Designs," IEEE Trans. Auto. Control, Vol. AC-26, pp. 75-92, February, 1981.